JOURNAL OF SOLID STATE CHEMISTRY 63, 216–230 (1986)

Studies of Phases in the $KNbO_3$–Nb_2O_5 System by High-Resolution Electron Microscopy and X-Ray Powder Diffraction

MONICA LUNDBERG AND MARGARETA SUNDBERG

Department of Inorganic Chemistry, Arrhenius Laboratory, University of Stockholm, S-106 91 Stockholm, Sweden

Received July 26, 1985; in revised form October 9, 1985

High-resolution electron microscopy and X-ray powder diffraction studies of specimens in the $KNbO_3$–Nb_2O_5 system have shown that, besides the previously reported layer structures $K_4Nb_6O_{17}$ and L-KNb_3O_8, there exist three different types of tetragonal tungsten–bronze-related structures as well as a block structure, $KNb_{13}O_{33}$, isostructural with the $NaNb_{13}O_{33}$ phase. The cell parameters and the structural relations to TTB are discussed. The first two TTB-related phases, superstructures of the TTB-type, are characterized by the formula $K_{2x}Nb_{2-x}^{A}(NbO)_x^{C}Nb_{10}O_{30}$, where $0 < x \leq 2$. H-KNb_3O_8 ($x = 2$), a high-temperature phase, exhibits a new mode of linking pentagonal columns in pairs. Various types of microstructures between the two TTB-related phases will be discussed. The third TTB-related phase can be described as $K_{10-5y}Nb_y^{A}Nb_{10}O_{30}$, where $0.8 < y < 1.25$. No pentagonal columns have so far been observed. In specimens prepared at $T > 1275$ K, the low-temperature modification L-KNb_3O_8, transforms in the solid state via a poorly crystallized phase to TTB-related structures. Some geometrical features of the L-KNb_3O_8, $KNb_{13}O_{33}$ structures and the TTB phase will also be presented.

Introduction

Several articles concerning phases in the K_2O–Nb_2O_5 system, have been published in the past.

Three phases, $K_4Nb_6O_{17}$, KNb_3O_8, and $K_6Nb_{44}O_{113}$, were observed by Reisman and Holtzberg (*1*) using differential thermal analysis. According to Nassau *et al.* (*2*) the cell parameters and the physical properties of the compounds $K_4Nb_6O_{17}$ and KNb_3O_8 suggested layer structures of mica type. This was later confirmed through X-ray single-crystal structure determinations by Gasperin and Le Bihan (*3*) and by Gasperin (*4*). Whiston and Smith (*5*) attributed identical stoichiometric compositions to these two phases. However, Weissenberg photographs of the compounds showed diffraction patterns of the tetragonal tungsten–bronze type (TTB), but one of these phases KNb_3O_8 gave superlattice spots. Additional phases were observed; among those one with the composition "$K_6Nb_{44}O_{113}$," which was assumed to be a solid solution of K_2O in the high-temperature form of Nb_2O_5, i.e., a "block structure."

Since the occurrence of TTB phases in the K–Nb–O system seemed doubtful, and in view of the results obtained from X-ray powder diffraction studies of TTB related phases in the KF–Nb_2O_5 system (*6*), high-resolution electron microscopy (HREM) and X-ray powder diffraction investigations of these systems were undertaken.

The tetragonal tungsten bronze structure

0022-4596/86 $3.00

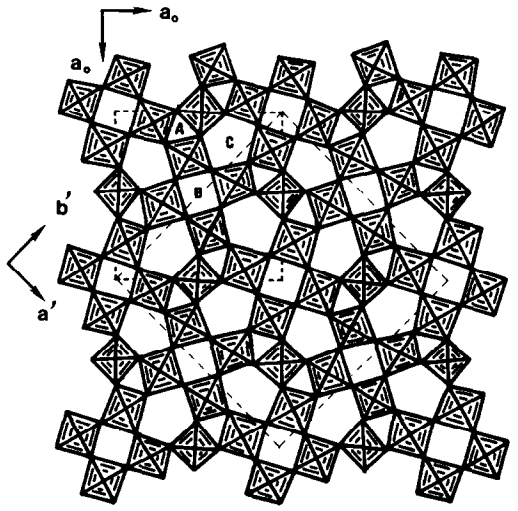

FIG. 1. The framework of octahedra in the TTB structure type projected along [001]. The three-, four-, and five-sided tunnels are marked A, B, and C, respectively. a_0 refers to the axis of the subcell. a' and b' represent the axes of the orthorhombic superstructure of H-KNb_3O_8.

was first determined for the compound K_xWO_3 by Magnéli (*7*). The polyhedral framework consists of WO_6 octahedra, linked by corners in such a way that three-, four-, and five-sided tunnels are created. The potassium atoms are located in the larger tunnels marked B and C in Fig. 1. Different types of TTB-related structures in the K-Nb-O system that contain exclusively pentavalent niobium atoms can be formed if an excess of Nb is added to the basic octahedral TTB framework, giving an oxygen-to-niobium ratio less than 3. Various types of TTB-related phases as well as a "block structure" will be reported in this article. The HREM results obtained for the oxide fluoride system will be published elsewhere.

Experimental

All specimens were prepared from Nb_2O_5 (Merck, optipure, purified of oxide fluorides in air at 1375 K) and $KNbO_3$ (obtained by heating appropriate amounts of K_2CO_3 (BDH, Laboratory reagents) and Nb_2O_5 in a platinum crucible at 1175 K for 2 days). The purity of the starting materials was checked by analysis of X-ray powder patterns.

The samples were thoroughly ground, pressed to pellets and kept in air at various temperatures between 1175 and 1395 K for periods of time varying between 2 and 50 days. The specific heating temperature of each sample is marked in the diagram (Fig. 2). The products were white and microcrystalline. The samples obtained were examined in a Guinier–Hägg powder diffraction camera and by electron-optical techniques. Unit cell dimensions were determined from the powder patterns and refined with the program PIRUM (*8*) using silicon as an internal standard (a/λ = 3.525176 (*9*)).

Specimens for the electron microscopy study were prepared in the following way. A small amount of a sample was crushed in an agate mortar and dispersed in *n*-butanol. Drops of this slurry were deposited on a perforated carbon film supported on a Cu-grid. The grid was then examined in a JEOL 200CX electron microscope, equipped with an ultrahigh-resolution top-entry goniometer stage and an image intensifier, which was connected on-line to an image processing system (Kontron IPS).

Electron diffraction patterns were recorded and used for identification of individual crystal fragments. High-resolution images (HREM images) of thin fragments were recorded (*10*). Most flakes were aligned with the short crystal axis (~3.9 Å) parallel to the electron beam.

Simulated images of some structure models have been calculated for crystal thicknesses of ~20, ~40, and ~60 Å, by using a local version of the SHRLI-suite of programs (*11*). The calculations have been made at different defocus values in the range −33 to -733 Å. The radius of the used objective aperture was 0.41 $Å^{-1}$.

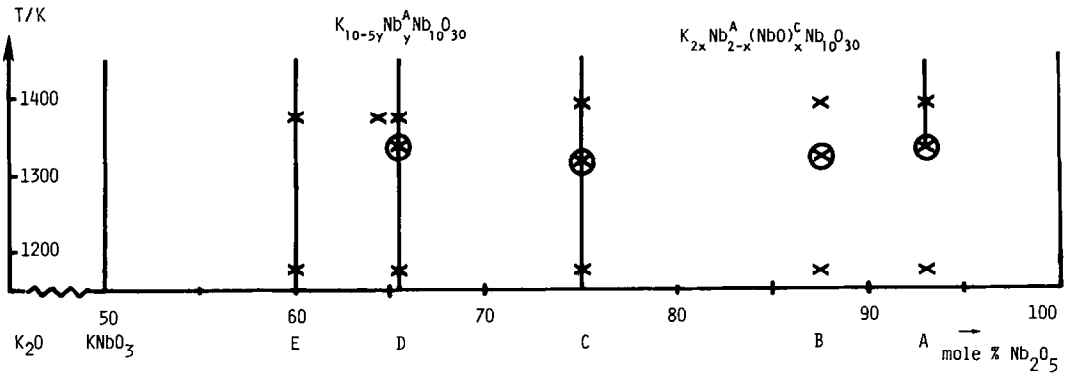

FIG. 2. A schematic phase diagram of $KNbO_3$–Nb_2O_5. Specimens examined both with electron-optical and X-ray powder techniques are marked ⊗. Samples studied only by X-rays are shown by ×. Nb^A and $(NbO)^C$ represent the type of Nb present at the A and C sites, respectively, as shown in Fig. 1.

Results of the X-Ray Studies

The phases discussed in this article are shown in the diagram (cf. Fig. 2) which does not purport to be a complete phase diagram of the region $KNbO_3$–Nb_2O_5. All refined unit cell parameters are given in Table I.

$KNb_{13}O_{33}$ (A)

$KNb_{13}O_{33}$ has been observed at $T > 1275$ K. The compound was never obtained as a single phase but could be identified in specimens which also contained H-Nb_2O_5 and a TTB-related phase. In spite of the fact that many reflections from H-Nb_2O_5 and $KNb_{13}O_{33}$ coincided, due to structural similarities, some reflections could be used to determine and refine the cell parameters. The final values are very close to those of the $NaNb_{13}O_{33}$ compound (*12*).

KNb_7O_{18} (B)

Specimens of gross composition

TABLE I

UNIT-CELL PARAMETERS (DERIVED FROM X-RAY POWDER DIFFRACTION DATA) FOR COMPOUNDS IN THE $KNbO_3$–Nb_2O_5 SYSTEM

Compound	*a* (Å)	*b* (Å)	*c* (Å)	*β*	*V* (Å³)	*M*(20) (Ref. (*18*))	*F* (Ref. (*19*))	*N*
(A) $KNb_{13}O_{33}$	22.479(3)	3.8370(5)	15.347(2)	91.07(2)	1323.5	12	12	83
(B) "KNb_7O_{18}"[a]	12.4909(4)	—	3.9629(3)	—	618.30	41	32	47
(C) H-KNb_3O_8[a]	12.5118(5)	—	3.9663(3)	—	620.90	36	22	42
(C) L-KNb_3O_8	8.9186(4)	21.206(1)	3.8053(1)	—	719.67	50	69	105
L-KNb_3O_8 (Ref. (*4*))	8.903(3)	21.16(2)	3.799(2)	—	715.7	—	—	—
(D) $K_{5.75}Nb_{10.85}O_{30}$	12.5788(3)	—	3.9833(1)	—	630.26	45	59	73
(E) $K_4Nb_6O_{17}$	7.816(6)	33.12(3)	6.480(3)	—	1677.4	7	8	31
$K_4Nb_6O_{17}$ (Ref. (*3*))	7.83(3)	33.21(10)	6.46(3)	—	1679.8	—	—	—

Note. Standard deviations are given in parentheses.

[a] Calculated for the TTB subcell. *N* number of lines used in the refinement.

KNb_7O_{18} mainly consisted of a TTB-related compound when heated at 1175 K. Small amounts of H-Nb_2O_5 were also present. After removing the reflection lines from H-Nb_2O_5, a tetragonal unit cell related to TTB was deduced and refined by indexing the remaining lines except three very weak ones. These unindexed lines belong to a superstructure of the TTB cell, which could not be refined, however. The HREM studies confirmed that these weak lines arise from the TTB superstructure.

Samples of this composition kept at temperatures above 1275 K contained $KNb_{13}O_{33}$ as a third phase. After seven weeks of heating the amount of H-Nb_2O_5 had decreased considerably. No changes of cell dimensions with temperature of preparation could be detected for the TTB-type phase.

KNb_3O_8 (C)

Reisman and Holtzberg (*1*) found that KNb_3O_8 melts incongruently at 1507 K, and according to Nassau *et al.* (*2*) the compound does not exhibit any phase transition below 1478 K. In the present investigation powder patterns were taken of samples that had been heated at 1175, 1315, and 1395 K for 7 weeks. The specimen obtained at 1175 K was single-phase and the powder photograph could be indexed by using the unit cell dimensions given by Gasperin (*4*). This phase will be designated L-KNb_3O_8 below. In the two samples heated at $T > 1275$ K an additional new phase, designated H-KNb_3O_8, appeared. After subtraction of all lines belonging to L-KNb_3O_8 the remaining lines could be indexed using a tetragonal cell very similar to the TTB unit cell. Careful visual study of the film revealed two very weak and diffuse reflections, which also could be indexed if an orthorhombic superlattice of TTB-type ($a' \sim b' \sim a_0\sqrt{2}$) was introduced. No reliable refinement of the superlattice parameters could be performed, but the same pattern of lines and intensity distribution have been observed previously for $KNb_6O_{15}F$ (*6*) with the cell dimensions $a = 17.686(3)$, $b = 17.580(5)$, and $c = 3.9629(5)$ Å. The refined subcell of H-KNb_3O_8 is listed in Table I.

$K_{5.75}Nb_{10.85}O_{30}$ (D)

Further to the $KNbO_3$ side in the diagram $K_{5.75}Nb_{10.85}O_{30}$ was prepared as a single-phase sample. All reflections in the powder photograph could be indexed with a unit cell of TTB-type. The refined cell parameters are larger than those obtained for H-KNb_3O_8 and the TTB-related phase in the specimen KNb_7O_{18}, which can be explained by structural differences (see below).

A sample of gross composition $K_6Nb_{10.8}O_{30}$ contained mainly this TTB related phase, but the X-ray powder pattern also indicated the presence of small amounts of $K_4Nb_6O_{17}$.

$K_4Nb_6O_{17}$ (E)

$K_4Nb_6O_{17}$ is a compound reported by several authors (*1–3*), although no accurate cell dimensions have been given. The powder pattern taken from a single-phase sample was indexed and the unit cell parameters were refined (Table I). The figures of merit ($M(20)$ and F) are quite low, probably due to the large unit cell and the somewhat broadened diffraction lines. The compound is very sensitive to water and transforms easily in humid air to $K_4Nb_6O_{17} \cdot 3H_2O$ (*3*).

Results of the Electron Microscopy Studies

$KNb_{13}O_{33}$ (A)

In the sample having the nominal composition $KNb_{13}O_{33}$, three phases H-Nb_2O_5, $KNb_{13}O_{33}$, and a TTB-related phase were identified by electron diffraction (ED) patterns from thin crystal fragments. These observations are in agreement with the X-ray results reported above.

Most ED patterns recorded of the H-

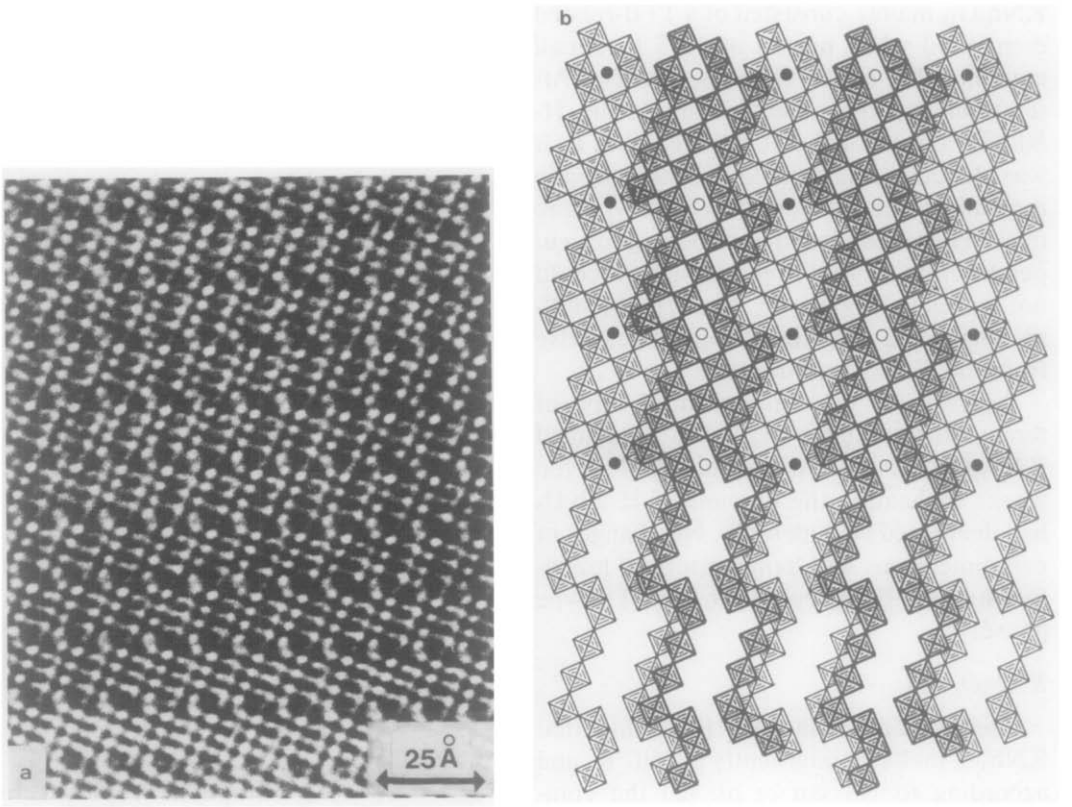

FIG. 3. HREM image of $KNb_{13}O_{33}$ projected along [010] (a). Structure model (b). The K atom positions in the large tunnels are shown.

Nb_2O_5 fragments, showed sharp reflection spots, which is indicative of a well-ordered structure.

The second phase was identified from the ED pattern, as well as from the micrograph shown in Fig. 3a, as isostructural with $NaNb_{13}O_{33}$ (*12*). The corresponding structure model projected along [010] is shown in Fig. 3b. There is good agreement between the observed image and the model. The black zigzag lines in the micrograph correspond to the crystallographic shear (*CS*) planes in the model. In the thinnest region of the flake (bottom Fig. 3a), the individual Nb atoms are resolved and can be identified as black spots. As can be seen from the model, blocks of (5 × 3 – 2) corner-sharing NbO_6-octahedra are joined in slabs by edge-sharing, so that large rectangular tunnels are formed. The slabs are regularly arranged at two levels and joined by edge-sharing (*CS*-planes). As can be seen from the micrograph, there is a faint black contrast dividing the rectangular tunnel into halves. This contrast can be interpreted as due to the K atoms, in analogy with what has been reported for the isostructural sodium compound (*13*). All fragments examined, showing this type of structure, were found to be very well-ordered.

The third phase was identified from the ED patterns as a superstructure of a TTB-related phase. The unit cell was three times the TTB cell (3 × TTB-type). The ED patterns also showed that twinning was frequent (Fig. 4). A 3 × TTB-type structure

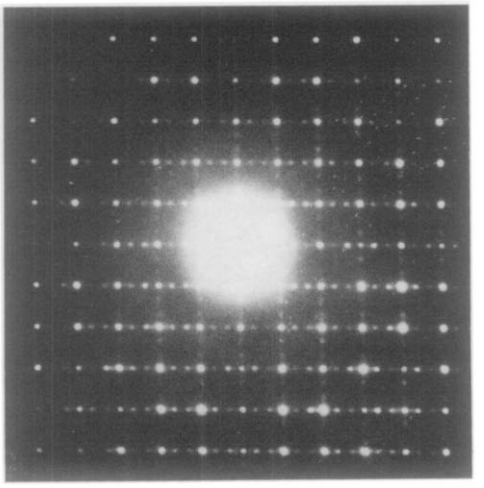

FIG. 4. ED pattern showing a twinned, tripled unit cell of TTB-type.

has previously been reported for $Nb_{16}W_{18}O_{94}$ (*14*). In this structure 4 out of 12 five-sided tunnels are occupied by —Nb—O—Nb—O— strings, so that 4 pentagonal columns (PCs) (*15*) are formed (see Fig. 6b).

Figure 5 shows a low-magnification micrograph taken of a thin crystal fragment, aligned with the short *c*-axis parallel to the electron beam. The image illustrates a fairly well-ordered 3 × TTB phase coexisting with domains (marked A) of another TTB-related phase. Images of the two regions are shown in higher magnification in Figs. 6a and 7a. There is fairly good agreement between the HREM image of the 3 × TTB-type phase in Fig. 6a and the structure model of $Nb_{16}W_{18}O_{94}$ in Fig. 6b. However, K atoms and some extra Nb atoms have to be inserted in the model (Fig. 6b) to obtain agreement with the supposed composition of the sample (see Discussion).

An interpretation of the domain structure in Fig. 7a is illustrated in Fig. 7b. The unit cell is now orthorhombic with two axes close to $a_0\sqrt{2}$ ($a_0 \sim 12.5$ Å) and the third axis ~3.9 Å. This structure is also a superstructure of the TTB-type. Two adjacent five-sided tunnels are occupied by —Nb—O—Nb—O— strings, so that two PCs are formed, which have one NbO_6 octahedron in common (Fig. 7b). This structural building unit, termed double-PC, is illustrated in Fig. 8. Four out of eight five-sided

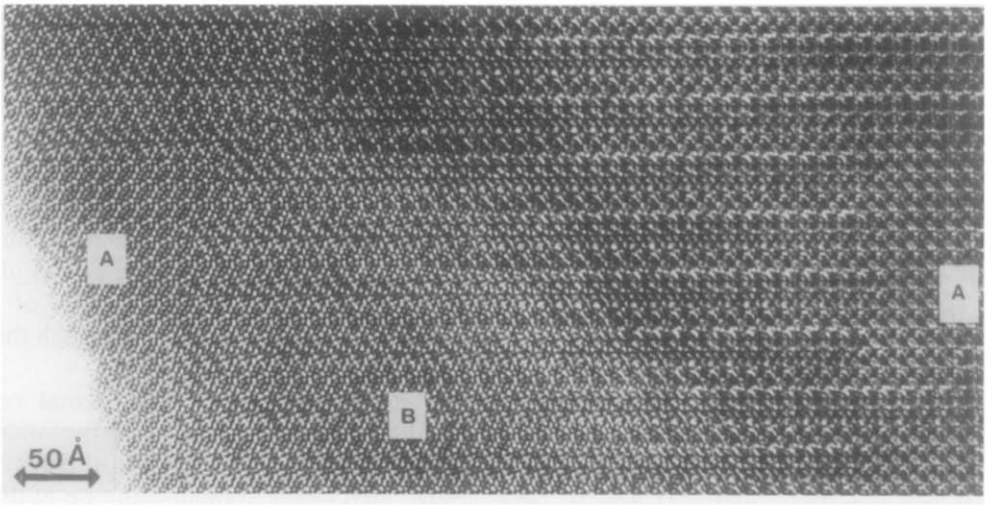

FIG. 5. Low magnification micrograph of a thin flake projected along [001], illustrating the TTB-related phases: H-KNb_3O_8 marked A and 3 × TTB marked B.

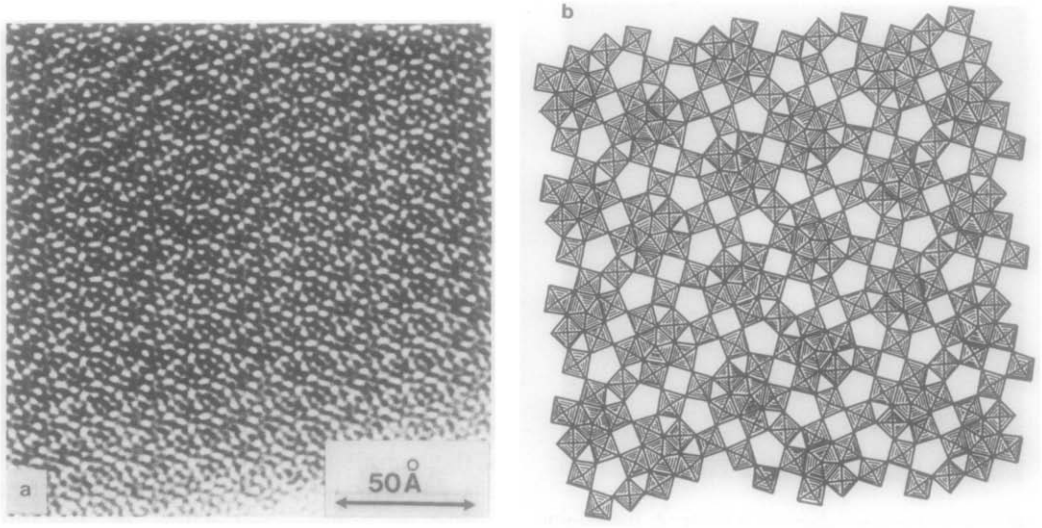

FIG. 6. HREM image of the 3 × TTB phase (a) and structure model of $Nb_{16}W_{18}O_{94}$ (b).

tunnels are filled with metal–oxygen strings, which define the stoichiometry $Nb_{24}O_{64}^{8-}$ of the niobium-oxygen framework. In order to obtain electroneutrality eight K atoms have to be inserted into the four- and five-sided tunnels in each unit cell. Below, this structure type will be denoted H-KNb_3O_8. Synthetic HREM images were calculated. The calculations were made with different defocus values and different crystal thicknesses. Some calculated images are shown in Fig. 7c. At a defocus value of −333 Å the observed and calculated images are in good agreement. The contrast is such that the K atoms do not appear at the tunnel sites. However, at the defocus −433 Å the contrast of the Nb and K atoms is almost similar.

KNb_7O_{18} (B)

The ED patterns and the HREM images of fragments from this sample revealed a wide range of TTB-related microstructures existing together with H-Nb_2O_5 and $KNb_{13}O_{33}$. Two examples are shown below.

The ED pattern inserted in Fig. 9a is of TTB-type but shows streaking and faint diffraction spots in the $[100]_{TTB}$ direction. The faint reflections indicate a superstructure with a unit cell three times that of TTB. The corresponding HREM image in Fig. 9a reveals microtwinning. An interpretation of the region marked by arrows in Fig. 9a is shown in Fig. 9b. In the $[110]_{TTB}$ direction, the structure can be described as composed of rows of one or more double-PCs as in H-KNb_3O_8. As seen in Fig. 9b these rows mostly end with a single PC at the twin boundary. There, the rows are mutually linked by corner-sharing to form the twin slabs. Note that the width of a slab consisting of one pair and two single PCs is of the same dimension as the *c*-axis of the $Nb_{16}W_{18}O_{94}$-type structure, although the arrangement of PCs is different.

Figure 10 illustrates the second rather similar microstructure. Here the slabs of double-PCs are wider than in the previous case. Two larger domains built up of the H-KNb_3O_8-type structure can also be seen. This type of domain structure is more fre-

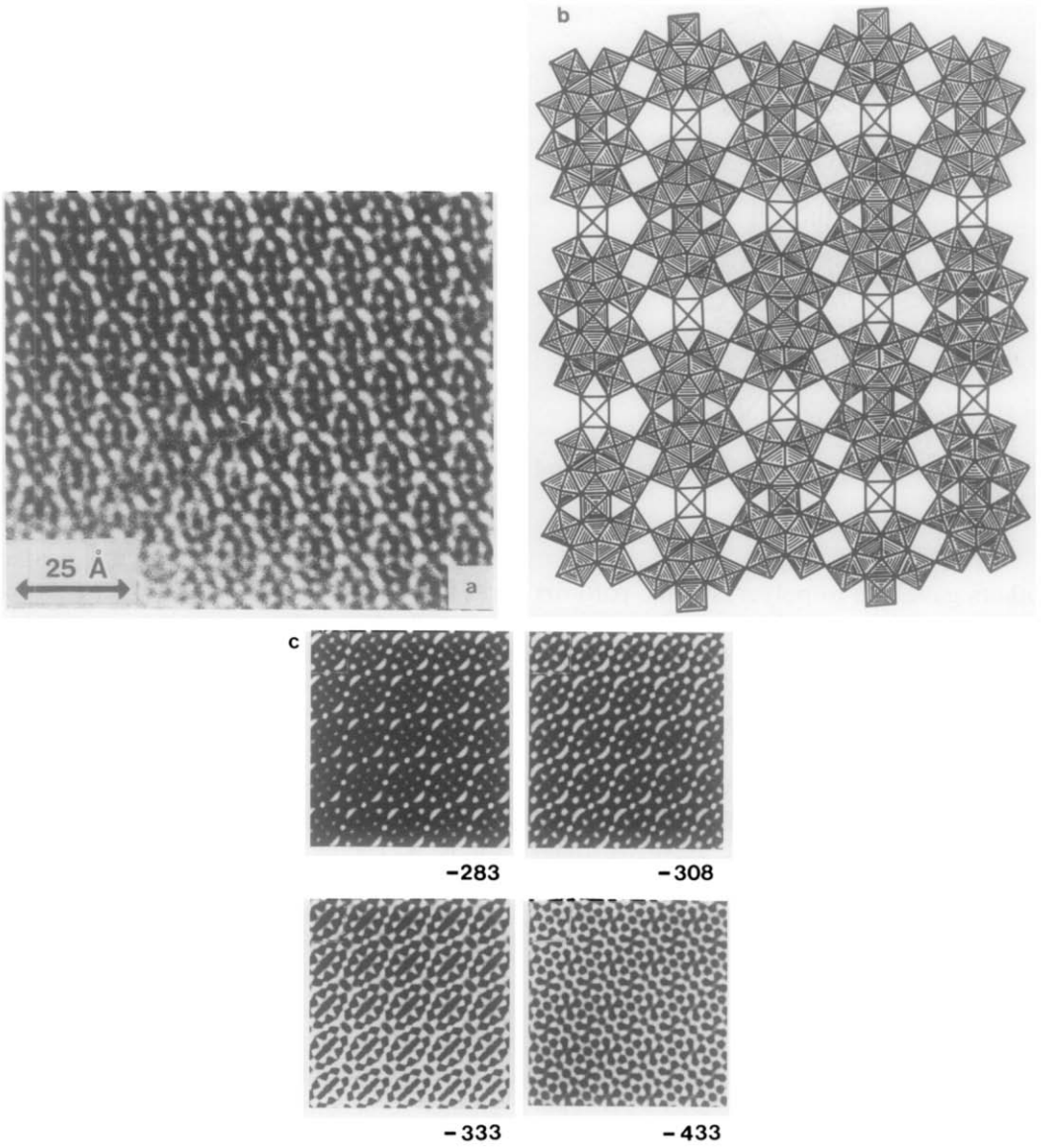

FIG. 7. HREM image illustrating the H-KNb_3O_8 phase (a). Structure model of H-KNb_3O_8 derived from the HREM image. The K atoms are not shown (b). Simulated images of the H-KNb_3O_8 model with K in four- and five-sided tunnels. Accelerating voltage 200 kV, objective aperture 0.41 $Å^{-1}$, C_s = 1.2 mm. Crystal thickness is 40 Å, defocus (−283–−433 Å) (c).

quently observed in this sample than in samples with the nominal composition $KNb_{13}O_{33}$.

KNb_3O_8 (C)

The results presented in this section are obtained from the sample with the nominal composition KNb_3O_8 heated at 1315 K for 3 weeks. Several types of ED patterns were recorded. Thus, the specimen was not a single phase. Some very thin flakes were identified as ordered L-KNb_3O_8, while

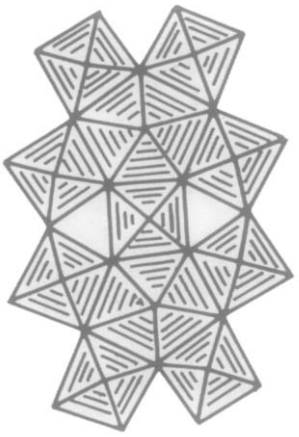

FIG. 8. A new mode of linking PCs, in the text called a double-PC.

others gave rise to polycrystalline patterns together with a very faint streaked pattern of L-KNb_3O_8. Several small fragments were identified as 3 × TTB-type crystals, Twinning was frequently observed in these fragments.

A few crystals also showed the ED pattern of H-KNb_3O_8. The electron-optical investigation indicated that L-KNb_3O_8 transforms in the solid state to TTB-related phases through an amorphous or poorly crystalline intermediate stage. One example is shown in Fig. 11.

$K_{5.75}Nb_{10.85}O_{30}$ (D)

The electron-optical results showed that this sample was a single phase of TTB-type. This is also in agreement with the X-ray diffraction results. No superstructure reflections could be observed in the ED pattern (Fig. 12). The corresponding HREM image is shown in Fig. 12.

With the composition $K_{5.75}Nb_{10.85}O_{30}$, 5.75 K, and 0.85 Nb must occupy some of the available tunnels. From previously known TTB structures of niobium oxides and the samples examined above, the extra Nb atoms and an equal amount of O atoms could be expected to enter the five-sided tunnels, forming pentagonal columns (PCs). However, in the HREM images, no PCs have so far been observed. It is therefore probable that the extra niobium atoms enter the three-sided tunnels. HREM images have been simulated for different models and conditions (see below). However, so far a definite clue to the location of these extra Nb atoms has not been reached. This study is still under way.

$K_6Nb_{10.8}O_{30}$

Two types of ED patterns were obtained from this sample. The first type showed fragments of $K_4Nb_6O_{17}$. Since the layer structure of this compound is known from previous X-ray diffraction work (*3*), it was not further considered here.

The second type of ED pattern indicated a TTB-type structure with no superstructure reflections. The structure is probably of the same type as in the previous sample ($K_{5.75}Nb_{10.85}O_{30}$).

Discussion

A tetragonal tungsten bronze structure of the K_xWO_3-type is not possible in the fully oxidized K–Nb–O system. The basic framework in such a TTB unit cell would have the composition $Nb_{10}O_{30}^{10-}$, which demands 10 K^+ ions to compensate the negative charge. Since the arrangement of the NbO_6 octahedra gives rise to only six interstices (marked B and C in Fig. 1) large enough to accommodate K^+ ions, no structure of this type with such a composition can be expected. However, a $KNbO_3$ phase exists but has adopted the perovskite structure type, which provides all the required interstices for the potassium ions.

Nevertheless a number of TTB-related phases have been obtained in this system. A common feature is that they all contain an excess of Nb, i.e., the oxygen-to-niobium ratio is less than 3. The extra Nb atoms can be introduced into the octahedral framework either as equal amounts of Nb and O in the five-sided tunnels (C in Fig. 1)

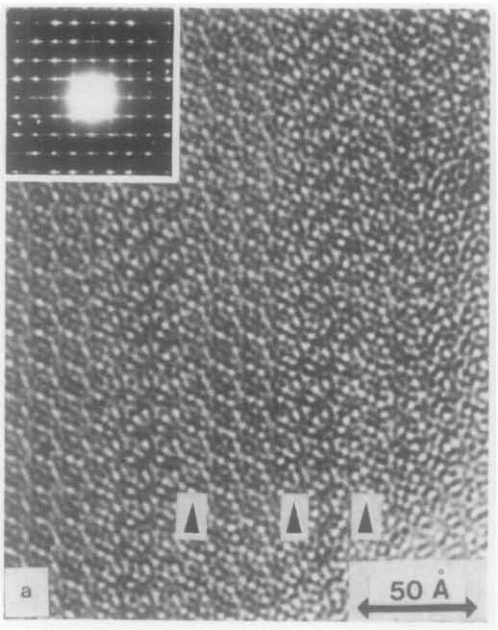

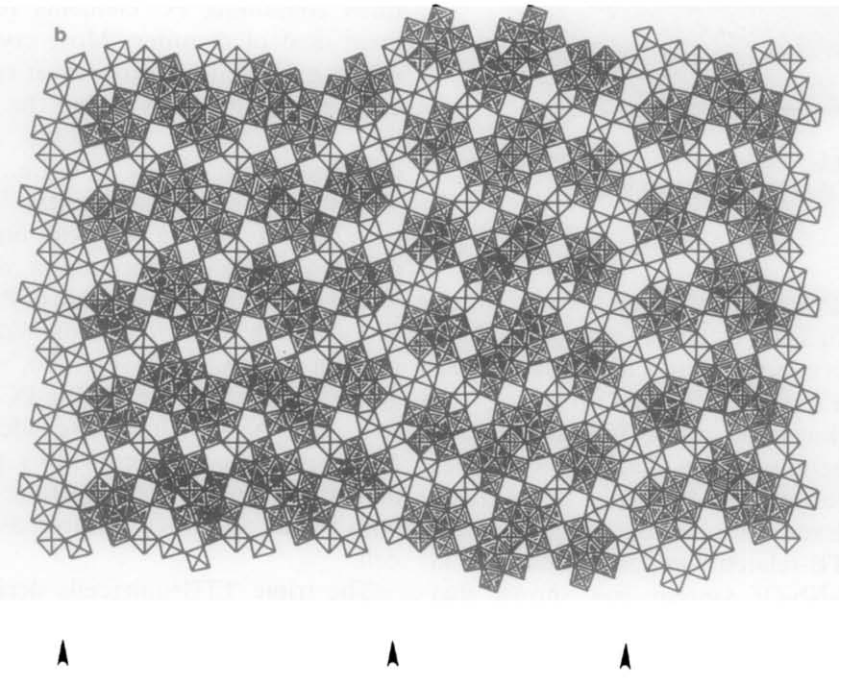

FIG. 9. HREM image with inset ED pattern illustrating a disordered microtwinned structure (a). Interpretation of the region marked by arrows (b).

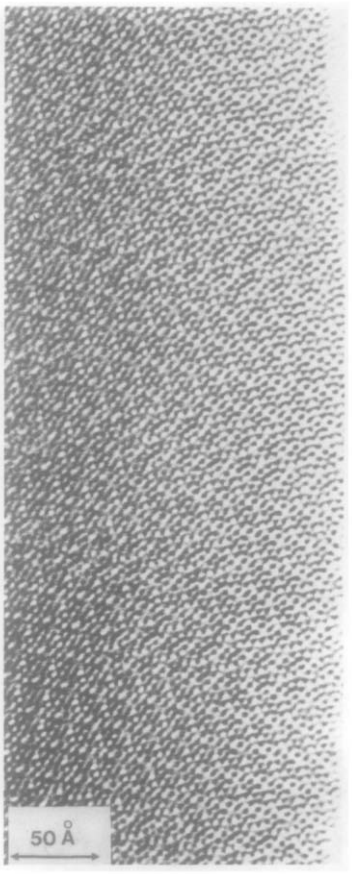

FIG. 10. Electron micrograph of a thin flake showing H-KNb_3O_8-type areas of different sizes.

creating PCs or as Nb atoms in the three-sided tunnels (A in Fig. 1) where nine oxygen atoms coordinate to a metal atom in the form of a tricapped trigonal prism.

According to the results from X-ray powder diffraction studies (Table I) both types of TTB-related phases coexist in the oxide system. Examination of the cell parameters of the TTB-related compounds obtained in the $KF–Nb_2O_5$ system has shown that when PCs are present in the structure the length of the c-axis is 3.96 Å and the cell volume is relatively constant (615–617 Å^3) (*6*). Thus, the potassium content does not affect the figures noticeably. Similar observations have been made for the two compounds H-KNb_3O_8 and "KNb_7O_{18}", whose HREM images show the occurrence of PCs (Figs. 9 and 10). The c-axes are 3.9663(3) and 3.9629(3) Å, with subcell volumes of 618 and 621 Å^3, respectively.

The third TTB-related phase, $K_{5.75}Nb_{10.85}O_{30}$, has a longer c-axis (3.9833 Å) and a larger unit cell volume (630 Å^3). No PCs have so far been observed in the HREM images, and it seems reasonable to assume that the excess niobium atoms (0.85/unit cell) are located in the three-sided tunnels (A). This is also in analogy with the single-crystal X-ray results from the $K_6Ta_{10.8}O_{30}$ compound, showing the excess 0.8 Ta/unit cell to be distributed over the three-sided tunnels (*16*). It should be noted, however, that if the 0.85 Nb are distributed over the fourfold position in a disordered way, the contrast will be very weak, as the simulated images show (Fig. 13).

HREM studies of the phases with structures containing PC elements revealed a great deal of disorder. Most crystal fragments exhibited intergrowth of two different types of PC links within the TTB matrix. One is the commonly occurring diamond-linked pair of PCs, i.e., two PCs sharing two octahedral corners. The other type consists of two PCs with one octahedron in common, forming a double-PC which represents a new mode of PC linking. These double-PCs are the dominating building unit in H-KNb_3O_8 (Fig. 7b), where single octahedra link the double-PCs. All the four- and the remaining five-sided tunnels are assumed to be occupied by potassium atoms, giving the composition KNb_3O_8, with a unit cell twice as large as the TTB cell.

The triple TTB unit cells derived from ED patterns of specimens with gross compositions equal to or larger than 75 mole% Nb_2O_5 indicate different kinds of superstructures. A similar diffraction pattern has been observed for the compound

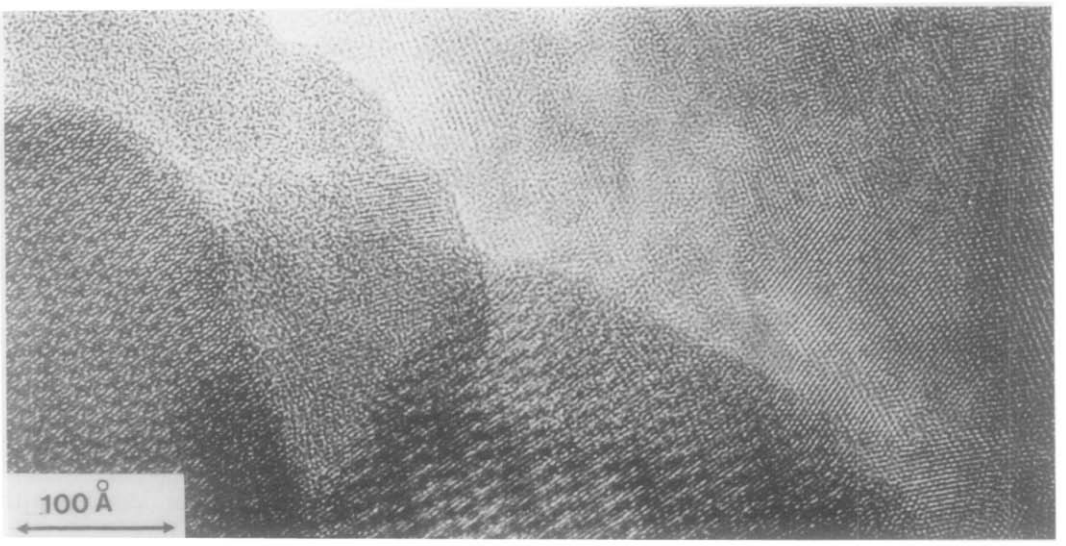

FIG. 11. Electron micrograph of a thin flake showing a fairly well-ordered 3 × TTB-type structure to the left-hand side, coexisting with a polycrystalline phase to the right.

$Nb_{16}W_{18}O_{94}$, where 1/3 of the pentagonal tubes, PTs (*17*), have been transformed into PCs arranged as diamond-linked doublets (Fig. 6b). The polyhedral framework contains 12 three-sided, 6 four-sided, and 8 five-sided tunnels per unit cell. Many alkali–transition-metal–oxide phases exhibit this type of structure.

A schematic drawing showing the differ-

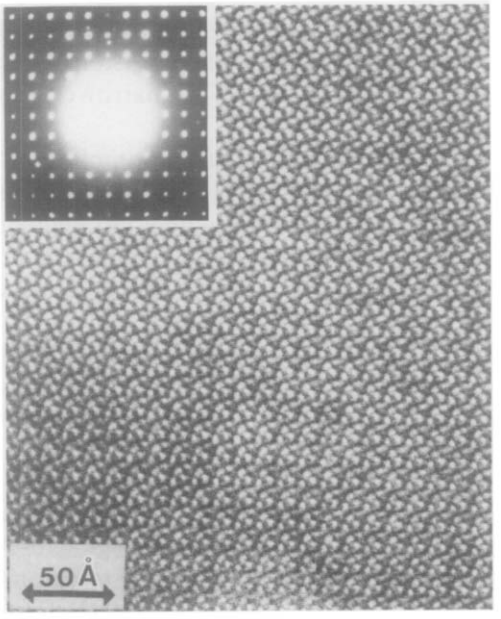

FIG. 12. HREM image of $K_{5.75}Nb_{10.85}O_{30}$ fragment, with the corresponding ED pattern inserted.

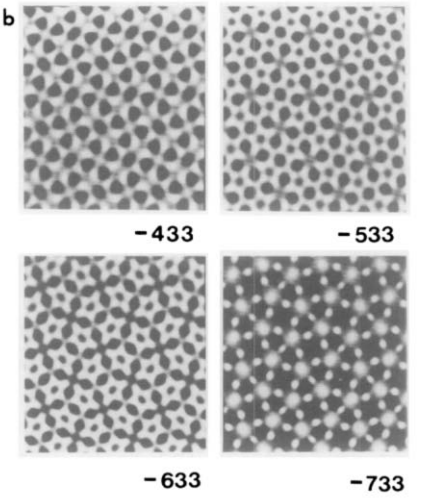

FIG. 13. Simulated images of the $K_{5.75}Nb_{10.85}O_{30}$ structure, with 0.85 Nb/unit cell distributed over the three-sided tunnels.

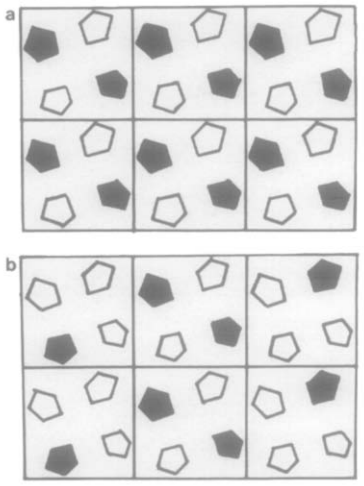

FIG. 14. A schematic drawing of the distribution of PCs in the structures H-KNb_3O_8 (a) and $Nb_{16}W_{18}O_{94}$ (b).

ence in distribution of PCs in the H-KNb_3O_8 and $Nb_{16}W_{18}O_{94}$ type structures is presented in Fig. 14.

In the present system it is not possible to synthesize a phase isostructural with $Nb_{16}W_{18}O_{94}$, which would have the theoretical composition $K_{18}Nb_{34}O_{94}$, since there are only 14 interstices in four- and five-sided tunnels available for the potassium atoms. A TTB-related compound with the same stoichiometry has been obtained, however, although not of the $Nb_{16}W_{18}O_{94}$ structure type. The ED pattern indicates a unit cell of normal TTB-type, and Nb is assumed to enter the prismatic sites as discussed above. The formula is then more conveniently written $K_{5.75}Nb_{10.85}O_{30}$.

In spite of this, the polyhedral framework of $Nb_{16}W_{18}O_{94}$-type has been observed in polyphasic samples higher in Nb_2O_5. Obviously there must be additional niobium inserted randomly in the basic atomic arrangement, very likely in the same nine-coordinated interstices discussed above (marked A in Fig. 1).

The same type of 3 × TTB diffraction pattern has also been obtained from a second type of superstructure appearing in the same crystal fragment as the former. The image can be interpreted as a mixture of PC and double-PC units. In these domains the unit cell can be described as having 4 or 6 out of 12 five-sided tunnels occupied by Nb and O strings (Figs. 9a and b).

The Nb-rich TTB phases containing PCs seem very often to be disordered. In order to express the compositions of this family of superstructures a general formula can be written as $K_{2x}Nb^{A}_{2-x}(NbO)^{C}_{x}Nb_{10}O_{30}$ ($0 < x \leq 2$). Nb^{A} indicates niobium at the A sites, and x is the amount of PCs in the subunit cell. However, larger domains with $x < 1.33$ have not yet been found.

It is also interesting to note that the maximal occupancy of five-sided tunnels with Nb–O strings in the TTB matrix does probably not exceed 50%, i.e., 6 PCs per unit cell. A denser filling may occur only locally in connection with twin planes and defects.

For less Nb-rich TTB phases a general formula for the unit cell content can be given as $K_{10-5y}Nb^{A}_{y}Nb_{10}O_{30}$, where y can vary between 0.8 and 1.25 at the most. However, the width of the nonstoichiometric region is likely to be narrower than these limits.

In the view of the distribution of the different types of TTB phases one may assume that the access to cavities large enough to accommodate K atoms determines whether PCs and/or Nb in tricapped trigonal prisms are present.

The variety of phases obtained in the Nb-rich part of the system bear interesting geometrical relations to each other which may be worth mentioning.

Three main types of structures can be discerned in the $KNbO_3$–Nb_2O_5 part of the diagram, namely those of $K_4Nb_6O_{17}$ and L-KNb_3O_8 which are layer structures, the nonstoichiometric, TTB-related $K_{10-5y}Nb^{A}_{y}Nb_{10}O_{30}$, $K_{2x}Nb^{A}_{2-x}(NbO)^{C}_{x}Nb_{10}O_{30}$ and $KNb_{13}O_{33}$ of block structure type. $K_4Nb_6O_{17}$

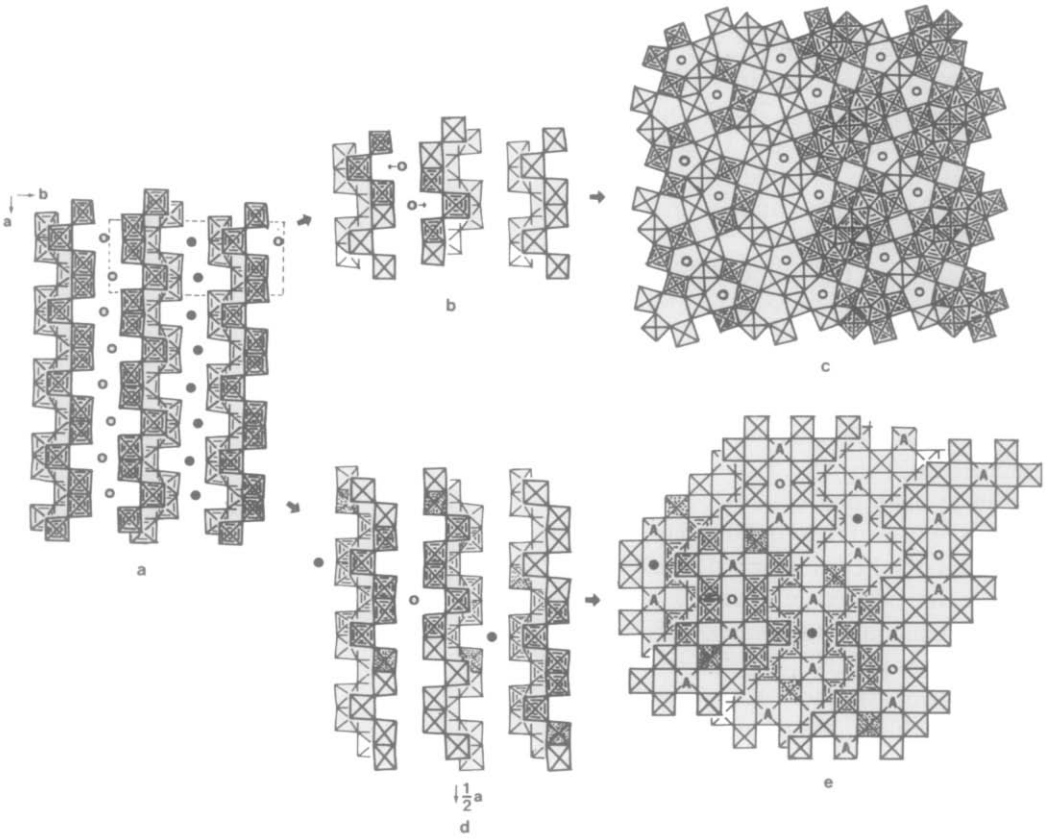

FIG. 15. Geometrical relationships between the L-KNb_3O_8, TTB, and $KNb_{13}O_{33}$ structures. L-KNb_3O_8 composed of layers of NbO_6 octahedra intercalated by K atoms (a). A unit of 6 NbO_6 octahedra (shaded) and 2 K atoms (b) is recognized in the H-KNb_3O_8 structure, completed with PCs in the right-hand part of the figure (c). The structure of $KNb_{13}O_{33}$ derived from units of 12 NbO_6 octahedra chosen as in (d) with every second layer shifted $\frac{1}{2}a$ of the L-KNb_3O_8 unit cell. Dotted octahedra are structurally equivalent and octahedra marked A are additional in order to complete the $KNb_{13}O_{33}$ framework (e).

will not be further discussed here, although some similarities occur between the two layer structure phases.

Geometrically L-KNb_3O_8 has certain relationships to both the TTB and the $KNb_{13}O_{33}$ structures but of different kinds.

The structure of L-KNb_3O_8 consists of layers of edge- and corner-sharing NbO_6 octahedra. The layers are interleaved by potassium atoms (Fig. 15a). The structure may also be looked upon as strings composed of repeat units of six NbO_6 octahedra, built up by corner-sharing among triplets, and two potassium atoms inserted at the same level as the apices of the octahedra (Fig. 15b). The so described units are mutually linked by edge-sharing octahedra. The K atoms are displaced in the direction of the arrows in Fig. 15b. The same unit can be recognized in the TTB, although additional octahedra (not shaded in Fig. 15c) are required to complete the structure. In the TTB structure the units are joined exclusively by corner-sharing (Fig. 15c) in such a

way that the arrangement of K atoms corresponds to the pattern of the five-sided, white tunnels appearing in HREM images of H-KNb_3O_8 (cf. Fig. 7b). It ought to be pointed out that only the K atoms in the five-sided tunnels are marked in Fig. 15c, although all four-sided tunnels are occupied by K atoms as well.

An alternative way of describing the Nb–O layers in the structure of L-KNb_3O_8 is to select a larger unit containing 12 octahedra (Fig. 15d). If every second layer is shifted by $\frac{1}{2}a$, the arrangement of NbO_6 octahedra becomes the same as that found in the structure of $KNb_{13}O_{33}$. However, one octahedron at each end of the L-KNb_3O_8 unit must be removed to avoid overlap, and two additional octahedra (marked A in Fig. 15e) must be introduced in order to obtain the three-dimensional framework of $KNb_{13}O_{33}$. The K atoms in $KNb_{13}O_{33}$ can be identified as being approximately at the same sites as every fourth K atom in the L-KNb_3O_8 structure.

Acknowledgments

We wish to thank Professor Lars Kihlborg for valuable comments on the manuscript and Mrs. Gunvor Winlöf for excellent help with the photographic work. This study has been supported by the Swedish Natural Science Research Council.

References

1. A. Reisman and F. Holtzberg, *J. Amer. Chem. Soc.* **77,** 2115 (1955).
2. K. Nassau, J. W. Shiever, and J. L. Bernstein, *J. Electrochem. Soc.* **116,** 348 (1969).
3. M. Gasperin and M.T. Le Bihan, *J. Solid State Chem.* **43,** 346 (1982).
4. M. Gasperin, *Acta Crystallogr. Sect. B* **38,** 2024 (1982).
5. C. D. Whiston and A. J. Smith, *Acta Crystallogr.* **19,** 169 (1965).
6. Li De-Yu, M. Lundberg, P.-E. Werner, and M. Westdahl, *Acta Chem. Scand. Ser. A* **38,** 813 (1984).
7. A. Magnéli, *Ark. Kemi* **1,** 213 (1949).
8. P.-E. Werner, *Ark. Kemi* **31,** 513 (1969).
9. C. R. Hubbard, H. E. Swanson, and F. A. Mauer, *J. Appl. Crystallogr.* **8,** 45 (1975).
10. J. C. H. Spence, "Experimental High Resolution Electron Microscopy," Clarendon Press, Oxford (1981).
11. M. A. O'Keefe and P. R. Buseck, *Trans. Amer. Crystallogr. Assoc.* **15,** 27 (1979).
12. S. Andersson, *Acta Chem. Scand.* **19,** 557 (1965).
13. J.-O. Bovin, L. Douxing, L. Stenberg, and H. Annehed, *Z. Kristallogr.* **168,** 99 (1984).
14. A. Sleight, *Acta Chem. Scand.* **20,** 1102 (1966).
15. M. Lundberg, Chem. Commun. Univ. Stockholm No. XII (1971).
16. A. A. Awadella and B. M. Gatehouse, *J. Solid State Chem.* **23,** 349 (1978).
17. M. Lundberg, M. Sundberg, and A. Magnéli, *J. Solid State Chem.* **44,** 32 (1982).
18. P. M. De Wolff, *J. Appl. Crystallogr.* **1,** 108 (1968).
19. G. S. Smith and R. L. Snyder, *J. Appl. Crytallogr.* **12,** 60 (1979).